THE ASTROPHYSICAL JOURNAL, 449:L23–L27, 1995 August 10

THE MORPHOLOGICAL MIX OF FIELD GALAXIES TO $m_I = 24.25$ MAGNITUDES ($b_J \sim 26$ MAGNITUDES) FROM A DEEP *HUBBLE SPACE TELESCOPE*[1] WFPC2 IMAGE[2]

SIMON P. DRIVER, ROGIER A. WINDHORST, AND ERIC J. OSTRANDER
Department of Physics and Astronomy, Arizona State University, Box 871504, Tempe, AZ 85287-1504
WILLIAM C. KEEL
Department of Physics and Astronomy, University of Alabama, Box 870324, Tuscaloosa, AL 35487-0324
AND
RICHARD E. GRIFFITHS AND KAVAN U. RATNATUNGA
Bloomberg Center for Physics and Astronomy, Johns Hopkins University, Box 182695, Baltimore, MD 21218-2695
Received 1995 December 21; accepted 1995 May 31

ABSTRACT

We determine the morphological mix of field galaxies down to $m_I \simeq 24.25$ mag ($m_B \sim 26.0$ mag) from a single ultradeep *Hubble Space Telescope* wide field planetary camera (WFPC2) image in both the V_{606} and the I_{814} filters. In total, we find 227 objects with $m_I \leq 24.5$ mag and classify these into three types: ellipticals (16%), early-type spirals (37%), and late-type spirals/irregulars (47%). The differential number counts for each type are compared with simple models in a standard flat cosmology. We find that both the elliptical and the early-type spiral number counts are well described by little-or-no-evolution models, but only when normalized at $b_J = 18.0$ mag. Given the uncertainties in the luminosity function (LF) normalization, both populations are consistent with a mild evolutionary scenario based on a normal/low rate of star formation. This constrains the end of the last *major* star formation epoch in the giant galaxy populations to $z \geq 0.8$.

Conversely, the density of the observed late-type/irregular population is found to be a factor of 10 in excess of the conventional no-evolution model. This large population might be explained by a modified *local* dwarf-rich LF and/or strong evolution acting on the *local* LF. For the dwarf-rich case, a *steep* faint-end Schechter slope ($\alpha \simeq -1.8$) is required, plus a fivefold increase in the dwarf normalization. For a purely evolving model based on a *flat* Loveday et al. LF ($\alpha \simeq -1.0$), a ubiquitous starburst of $\Delta I \sim 2.0$ mag is needed at $z \simeq 0.5$ for the *entire* late-type population. We argue for a combination of these possibilities, and show that for a steep Marzke et al. LF ($\alpha \simeq -1.5$) a starburst of ~1.3 mag is required at $z \simeq 0.5$ in the entire late-type population, or ~2.0 mag in ~20% of the population.

Subject headings: galaxies: elliptical and lenticular, cD — galaxies: evolution — galaxies: irregular — galaxies: luminosity function, mass function — galaxies: spiral

1. INTRODUCTION

Over recent years the nature of faint blue field galaxies observed in deep CCD images has been addressed through two main techniques: galaxy number counts and faint redshift surveys (Koo & Kron 1992, hereafter KK92). While differential galaxy counts in short wave bands show a remarkable excess of faint blue galaxies (Kron 1982; Broadhurst, Ellis, & Shanks 1988, hereafter BES), the current faint redshift surveys show a distribution which is well fitted by the standard no-evolution model (although the luminosity function [LF] normalization is incorrect). This conundrum has given rise to a large number of sophisticated models, most of which introduce an evolutionary process (see Phillipps & Driver 1995, for example, and references therein).

Recent papers from the *Hubble Space Telescope* (*HST*) Medium Deep Survey (MDS) have now introduced an additional constraint: the *morphological* classification of faint field galaxies at *HST*'s resolution of 0.″1 FWHM. Casertano et al. (1995, hereafter CRGINOW) give the differential galaxy number counts for *HST* bulges and disks separately from the prerefurbished wide-field planetary camera (WFPC) MDS database (13,500 galaxies with $m_{I_{F785LP}} < 21$ mag). Griffiths et al. (1994), Driver, Windhorst, & Griffiths (1995b, hereafter DWG) and Glazebrook et al. (1995a, hereafter GL95a) use WFPC2 data to extend the morphological classification of faint field galaxies to $m_I \simeq 22.0$ mag. They find that about one-third of the total differential number counts with $m_I \leq 22.0$ mag consist of Sd/irregular galaxies, far more than expected based on estimates of the local Sd/Irr population. About 35% of this population show clear signs of star formation (cf. DWG). The remaining contribution to the number counts at $m_I \sim 22.0$ mag consists of normal ellipticals and spirals, which are well fitted by standard mild or no-evolution models (DWG; GL95a). Here we analyze the 24-orbit WFPC2 exposure of Windhorst & Keel (1995, hereafter WK), and extend the morphological classification of faint field galaxies to $m_I \simeq 24.25$ mag ($m_B \simeq 26$ mag).

2. WFPC2 DATA REDUCTION AND IMAGE ANALYSIS

This single deep WFPC2 field has a total of 5.7 hr exposure in both V_{606} and I_{814}, and was reduced as described in WK, DWG, and CRGINOW (i.e., superbiases, superdarks, super–sky flats, and bad-pixel maps from the MDS). Cosmic-ray removal was achieved by the technique described in Windhorst, Franklin, & Neuschaefer (1994c) updated for WFPC2.

[1] Based on observations with the NASA/ESA *Hubble Space Telescope* obtained at the Space Telescope Science Institute, which is operated by AURA, Inc., under NASA contract NAS 5-26555.

[2] Send preprint requests to spd@starburst.la.asu.edu.

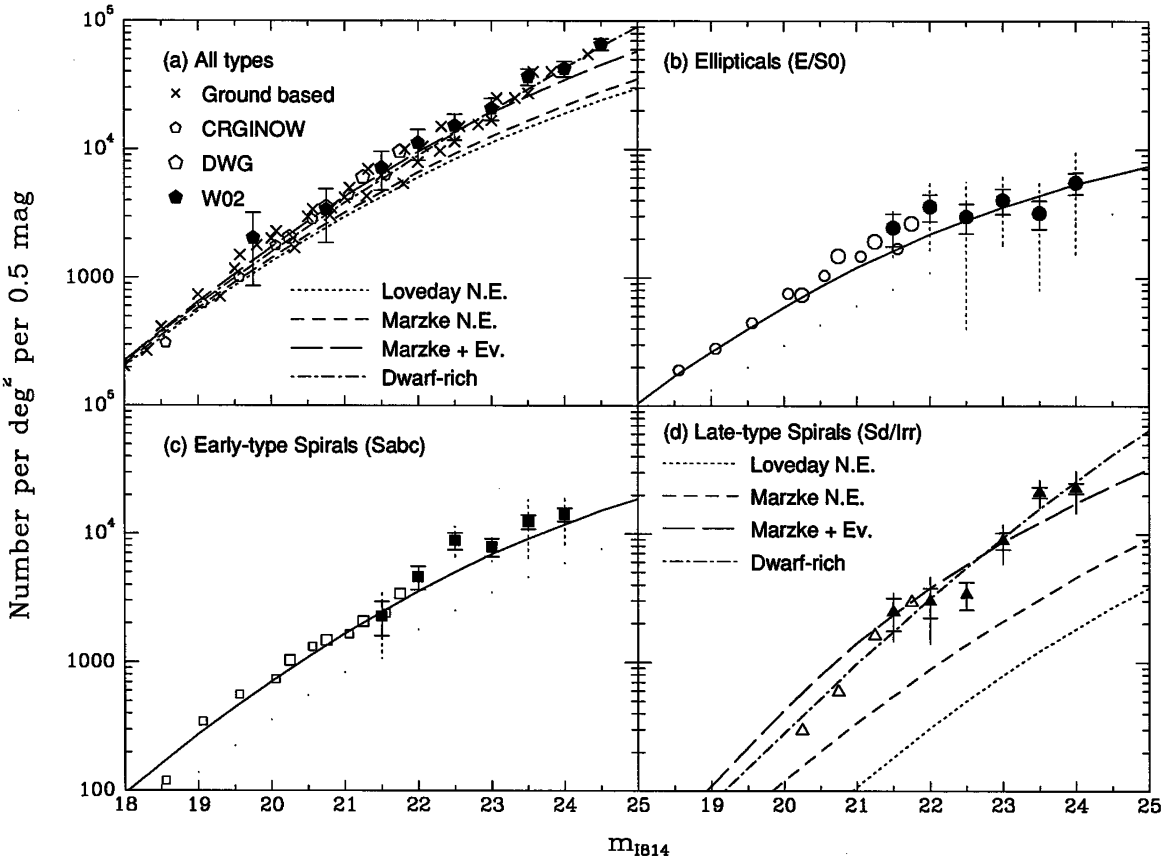

FIG. 2.—Differential *I*-band number counts for (*a*) all galaxies, (*b*) ellipticals, (*c*) early-type spirals, and (*d*) late-type spirals/irregulars. The open symbols without error bars are from the larger but shallower *HST* surveys of CRGINOW (*small symbols*) and DWG (*large symbols*). The solid symbols with error bars represent our new *HST* WFPC2 data. The errors are $\sqrt{n/N}$, where n represents the number of objects and N the number of classifiers. The vertical dotted lines represent the range of agreement between classifiers, and give a conservative upper limit to the true errors. The lightly dotted lines in (*b*) and (*c*) represent the *un*normalized LF predictions (see text).

Figure 1 (Plate L4) is a color plate of the entire WFPC2 field. The planetary camera (PC) image was not used for the current study because of its lower surface brightness (SB) sensitivity. Initial object positions and total magnitudes were measured using isophotal object-finding software of Ratnatunga et al. (1995). All objects were examined by eye and recombined or split as necessary. This yields two object catalogs in V and I which are complete, based on the turnover of the counts, to $m_I \simeq 25.50$ and $m_V \simeq 26.75$ mag. In total, we find ~600 and ~850 objects, respectively, down to these limits in the three wide-field camera CCDs, implying a surface density of 4.4×10^5 and 6.2×10^5 objects deg^{-2}. In this paper we consider only those galaxies with $m_I \leq 24.25$ mag, i.e., 1.25 mag above our formal completeness limit. Hence, for low SB galaxies, we become incomplete for objects with isophotal extent $\gtrsim 7$ arcsec^2, and for luminous bulges at $z \gtrsim 1.0$. We find no objects down to $m_I = 24.25$ mag larger than 1.0 arcsec^2, and the current faint redshift surveys—which extend to $m_{bJ} = 24$ mag—find very few galaxies with $z \gtrsim 1$ (Glazebrook et al. 1995b), although these surveys may also suffer SB selection effects. An in-depth discussion of the completeness of *HST* images is given by Neuschaefer et al. (1995).

3. *HST* GALAXY NUMBER COUNTS AS A FUNCTION OF TYPE

Figure 2*a* shows the differential number counts for the *HST* *I* band compared to ground-based data (Tyson 1988; Lilly, Cowie, & Gardner 1991; Driver 1994; Neuschaefer & Windhorst 1995). Note the good agreement between the ground-based counts and our deep *HST* counts, as well as with previous *HST* *I*-band counts (DWG and the WFPC I_{F785LP}-band counts of CRGINOW). The conversion from WFPC2 F814W to Cousins I_C is derived from Holtzman et al. (1995) and Bahcall et al. (1994) as $I_{814} = I_C + 0.05$ mag, assuming a mean galaxy color of $(V-I)_C \simeq 1.5$ (Driver 1994) and $(V_{606} - I_{814}) \simeq 1.0$ mag (DWG). Our deep WFPC2 *I*-band counts extend the ground-based counts in Figure 2*a* with a best-fit slope of 0.34 ± 0.03 for 22.0 mag $< m_I <$ 25.5 mag. The *V*-band counts have a slope of 0.38 ± 0.03 for 23.0 mag $< m_V <$ 27.0 mag, implying a trend toward bluer $(V-I)$ colors at fainter magnitudes. At $m_I \simeq 21.5$ mag, the mean field galaxy $(V-I)$ color is 1.3 ± 0.3 ($1\,\sigma$), changing to 0.8 ± 0.3 at $m_I \simeq 25.0$ mag, and shows little correlation with galaxy type (see DWG). Hence, we do not use color to classify; moreover, redshifts and *K*-corrections at $I \simeq 24$ mag ($b_J \simeq 26$) are unknown.

Following the methods in DWG, we did the photometry for the 227 objects with *total* flux $m_I \leq 24.5$ mag, resulting in an accuracy of ± 0.1 mag (cf. DWG). The objects were classified into ellipticals, early-type spirals, and late-type spirals/irregulars using both the *V*- and *I*-band morphology and light profiles. As in DWG, the distinction between "early" (Sabc) and "late" (Sd/Irr) is based on a combination of their mea-

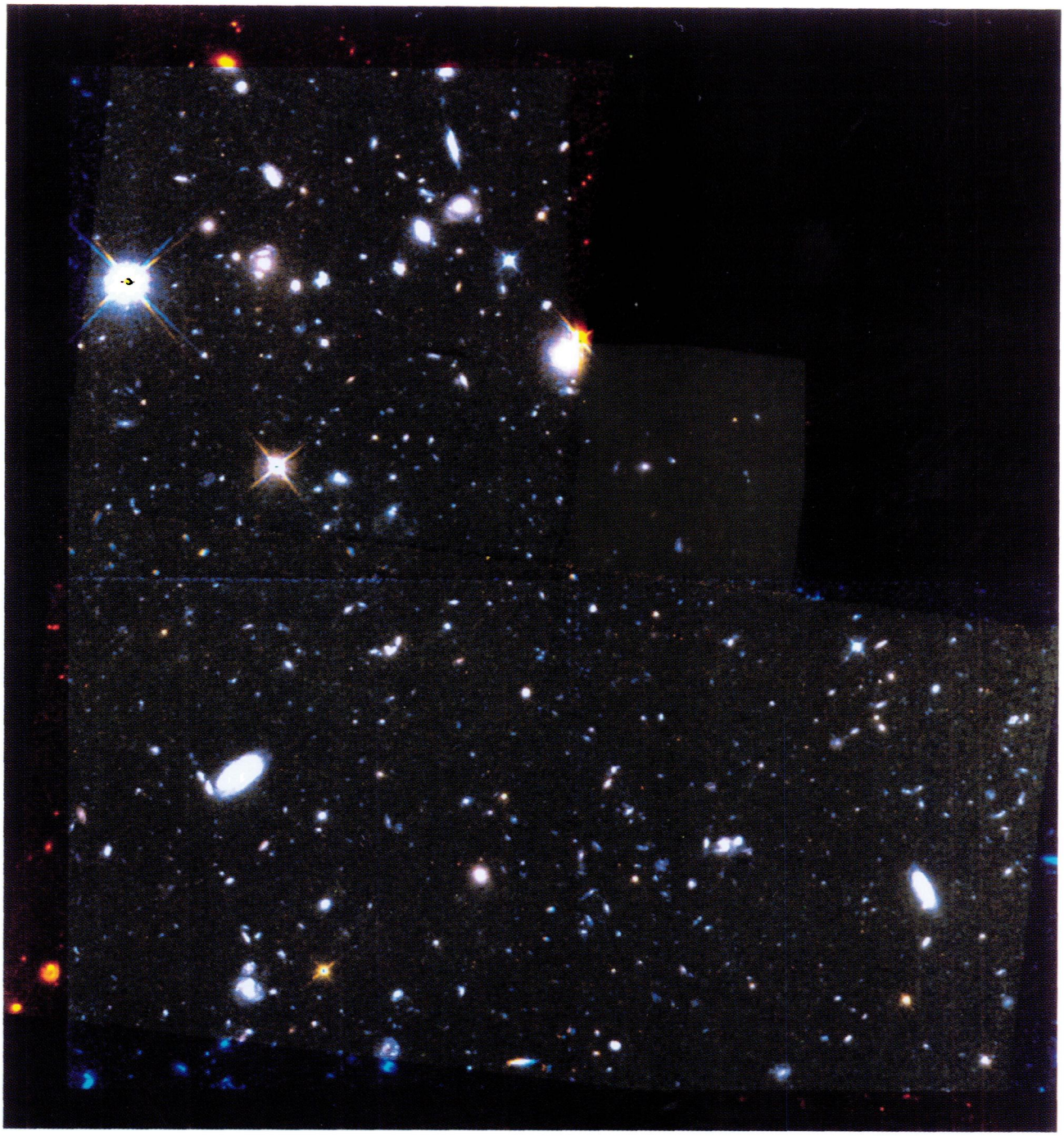

FIG. 1.—This color image shows the 5.7 hr WFPC2 images in both the I_{814} and the V_{606} filters surrounding the weak radio galaxy 53W002 at $z = 2.390$ (Windhorst & Keel 1995). Images in V, $(V + I)/2$, and I are shown in the blue, green, and red guns, respectively. A total of 600 objects in the I and 850 objects in the V frames have been detected down to $m_I \simeq 25.5$ and $m_V \simeq 26.75$ mag in 0.00136 deg^2, implying a surface density of 4.4×10^5 and 6.2×10^5 deg^{-2} in I and V, respectively. The V and I images have a 6°.73 difference in *HST* roll angle, leading to apparently extreme object colors at the CCD edges.

DRIVER et al. (see 449, L24)

TABLE 1

AGREEMENT BETWEEN THE FOUR INDEPENDENT EYEBALL CLASSIFIERS AS A FUNCTION OF FLUX

	MAGNITUDE INTERVAL		
AGREEMENT	$I < 20.25$	$20.25 < I < 22.25$	$22.25 < I < 24.25$
4 of 4.....	9 (75%)	12 (36%)	53 (36%)
3 of 4.....	3 (25%)	12 (36%)	54 (37%)
2 of 4.....	0 (0%)	9 (28%)	39 (27%)

sured central SB and a careful assessment of their measured light profiles, bulge-to-disk ratios, and gray-scale images (see DWG for an example of the Hubble sequence at $m_I \simeq 21.5$ mag). The final assigned galaxy types are the consensus of four *independent* classifiers (S. P. D., R. A. W., E. J. O., and W. C. K.) and were determined by averaging the number of galaxies in each class and in each magnitude interval (as opposed to defining an average or most likely class for each object individually). The consistency between the four independent classifiers is summarized in Table 1. Note that the scatter in the interval 22.25 mag $< m_I <$ 24.25 mag is equivalent to that in 20.25 mag $< m_I <$ 22.25 mag.

Figure 2 shows the differential number counts for (*b*) ellipticals/S0, (*c*) early-type spirals, and (*d*) late-type spirals/irregulars. Figure 2 also includes the WFPC data of CRGINOW (for all galaxies, ellipticals and spirals) for $I \leq 21.0$ mag, and the WFPC2 data of DWG for $I \leq 22.0$ mag. Errors are derived from assuming Poisson statistics. The formal errors ($\sqrt{n}$) are shown by solid error bars. Vertical dotted lines indicate the *total* range covered by the four independent classifiers, and are a *conservative* estimate of the true classification errors. Where our new data overlap with those of CRGINOW and DWG, there is good agreement within the formal errors. The largest errors occur for the E/S0 galaxies, where the statistics are smallest and which are the hardest to recognize—even with *HST*—because of their small scale lengths (Mutz et al. 1994; Windhorst et al. 1994a, b). The level of agreement between our four independent classifiers down to $I \leq 24.25$ mag is comparable to that achieved by DWG for $I \leq 22.0$ mag. In Table 1 the disagreement between classifiers is exaggerated because the data are binned into a *small* number of classes. For example, if two classifiers agree on one galaxy as S0 and two as Sa, this might be considered a reasonable agreement, but because we bin objects into three classes, such disagreements seem more significant. Table 2 shows the morphological mixes observed at various flux limits. The bright end of our *HST* sample agrees well with the faint end of the DWG sample, and the bright end of the DWG sample agrees well with the local fractions (Shanks et al. 1984).

We applied the bulge or disk-fitting algorithms of CRGINOW to provide an *independent* automated classification for all 227 objects into ellipticals or spirals, as shown in Table 2. While this algorithm cannot distinguish between mid- and late-type spirals, the fractions of brighter galaxies (21 mag $\leq I <$ 23.0 mag) classified into bulges and disks *by the algorithm* are 30% and 70%, respectively, while for those classified *by eye* they are 32% and 68%. At the faint end (23 mag $\leq I <$ 24.5 mag) the correspondence is still satisfactory: the bulge and disk fractions are 21% and 79% *by the algorithm*, and 14% and 86% *by eye*, respectively. Software to achieve two-dimensional simultaneous bulge *plus* disk fits is under development and will be described in a subsequent paper

TABLE 2

COMPARISON OF THE MORPHOLOGICAL MIX OF FIELD GALAXIES BY VARIOUS GROUPS

Source	Magnitude	E/S0 (%)	Sabc (%)	Sd/Irr (%)	Unclassified (%)
MGHC (CFA1)[a]	$m_Z < 14.5$	35	54	10	1
MGHC (CFA2)[a]	$m_Z < 15.5$	42	48	8	2
Shanks et al. 1984	$m_{b_J} < 16.0$	43	45	12	0
Griffiths et al. 1994	$m_I < 22.25$	19	44	13	25[b]
DWG bright	$m_I \sim 20.25$	36	50	14	0
GL95a bright	$m_I = 20.25$	31	48	21	0
DWG faint.....	$m_I \sim 21.75$	28	35	31	6
GL95a faint.....	$m_I = 21.75$	29	35	33	3
Current, bright, eye	$m_I \sim 22.00$	32	38	30	0
Current, bright, automated[c].....	$m_I \sim 22.00$	30	70		0
Current, faint, eye.....	$m_I \sim 24.00$	14	30	56	0
Current, faint, automated[c].....	$m_I \sim 24.00$	21	79		0

[a] The mix for the CFA1 and CFA2 samples were estimated from Fig. 1 of MGHC.

[b] Griffiths et al. 1994 note that a significant fraction of the unclassified galaxies were classified as S0 by one of their two classifiers.

[c] Automated classifications were determined from the profile fits of CRGINOW and Ratnatunga et al. 1995. This algorithm cannot distinguish between Sabc's and Sd/Irr's, so *all* disk-dominated galaxies are listed together.

(Ratnatunga et al. 1995). A comprehensive spectroscopic survey is also in progress for the DWG sample (Driver et al. 1995a) and will help confirm these classifications.

We conclude that we have—within the limits of the available data—a consistent picture of the trend of morphological mix with apparent magnitude. Figure 2 and Table 2 show that the galaxy mix at *faint* magnitudes is significantly different from the local values, with a far higher proportion of late-type galaxies seen at the *HST* limit.

4. MODEL FITTING

To model the differential number counts for each galaxy type separately, we adopted three independent luminosity functions (LFs), a standard flat cosmology ($\Lambda = 0$, $\Omega = 1$, and $H_0 = 50$ km s^{-1} Mpc^{-1}; cf. Phillipps, Davies, & Disney 1990), and *K*-corrections (cf. Driver et al. 1994). The modeling process is described in DWG. For *nonevolving* E/S0 and Sabc galaxies, we parameterized the *observed* luminosity distributions (LDs) from Marzke et al. (1994, hereafter MGHC) using their tabulated values for E/S0 ($M_B^* = -20.5$ mag, $\alpha = -0.9$, $\phi_* = 1.14 \times 10^{-3}$ Mpc^{-3}) and for Sabc ($M_B^* = -20.3$ mag, $\alpha = -0.8$, $\phi_* = 1.74 \times 10^{-3}$ Mpc^{-3}). The LFs were exponentially cut off at $M_B^{\rm cut} = -17.5$ mag [i.e., the standard Schechter 1976 function was multiplied by exp $(-10^{0.4(M - M^{\rm cut})})$]. To convert the observed *B*-band LDs to the *I* band, we adopted the following mean colors (Windhorst et al. 1994b) at $z = 0$: $(B - I)_{\rm E/S0} \simeq 2.3$, $(B - I)_{\rm Sabc} \simeq 1.9$, and $(B - I)_{\rm Sd/Irr} \simeq 1.4$ mag. The LF models were normalized to the observed number counts for all types at $m_{b_J} \simeq 18$–20 mag (cf. KK92), resulting in a uniform 0.3 dex increase in numbers for each type. As discussed in DWG, this discrepancy in normalization arises from the observed steep galaxy counts at $b_J \lesssim 17$ mag (see also Shanks et al. 1989). In line with standard practice (cf. KK92), we normalize our models at $b_J \sim 18$ mag, intended to represent a sufficient distance to cover a homogeneous volume (i.e., $z \sim 0.15$ or $b_J \sim 18$–20 mag), but at a low enough redshift that strong evolution has not yet occurred.

Figures 2*b* and 2*c* show the model predictions for elliptical

and early-type spiral galaxies, compared with our *HST* data. The models mimic the observed distribution rather well, implying—with the adopted LF normalization—little luminosity evolution (LE) for both the elliptical and the early-type spiral populations. Note that the lightly dotted lines in Figures 2*b* and 2*c* represent the predictions from the *un*normalized local LFs, which would imply stronger evolution for the early-type populations. To model the late-type/irregular population, three alternate LFs were used in the following four models:

(a) A *no-evolution* prediction based on the Loveday et al. (1992, hereafter LPEM) LD for late-type galaxies [$M_B^* = -18.5$ mag, $\alpha = -1.1$, ϕ_*(Sd/Irr) = 7.0×10^{-4} Mpc^{-3}; cf. DWG].

(b) A *no-evolution* prediction based on the MGHC LD for late-type galaxies ($M_B^* = -20.3$ mag, $\alpha = -1.5$, $\phi_* = 2.5 \times 10^{-4}$; DWG).

(c) An *evolving* model (Phillipps & Driver 1995) that mimics a ubiquitous starburst in the Sd/Irr galaxy population at $z \simeq 0.5$, after which their luminosity declines exponentially with time (i.e., $\Delta m \propto \beta[1 - (1 + z)^{-3/2}]$ for $\Omega = 1$ with M_B^*, α, and ϕ_*(Sd/Irr) from model (a) or model (b), and β = free).

(d) A *no-evolution* dwarf-rich model with $\alpha = -1.8$ (cf. Driver et al. 1994). The normalization is *increased* until a fit is found to the data [$M_B^* = -18.0$ mag, $\alpha = -1.8$, and ϕ_*(Sd/Irr) = free].

For models (a) and (b), the late-type/irregular parameters listed above were taken *directly* from DWG. Figure 2*d* shows that they grossly underpredict the observed late-type/irregular population. For model (c), the amount of luminosity evolution required for the *entire* late-type population was found to be $\Delta m \sim 2.0$ mag at $z \simeq 0.5$ to match the counts with the LPEM LF, and ~1.3 mag with the MGHC LF. The required ~1.3 mag increase in luminosity for the *entire* late-type galaxy population is equivalent to a ~2.0 mag increase in ~20% of the population. For the dwarf-rich model (d), a local normalization of $\phi_* \sim 3.5 \times 10^{-2}$ Mpc^{-3} was required to match the counts, which is a factor of 5 greater than that of LPEM (not including the additional 0.3 dex normalization). Such a dwarf LF, however, is inconsistent with the faint redshift surveys, as it predicts too many low-redshift objects (Driver 1994; Phillipps & Driver 1995).

Figure 3*a* (Plate L5) compares the best-fit individual LFs adopted for each galaxy type. Figure 3*b* shows the conventional differential number counts with the contribution from each galaxy type indicated by the best-fit model lines from Figures 2*a*–2*d*. Figure 3*c* shows the observed LD, which reflect the actual relative numbers that would be observed in a *magnitude-limited* survey (assuming equal selection effects for all types). Figure 3*d* shows the *normalized* differential galaxy number counts, which emphasizes the differences between the models and the data.

5. DISCUSSION AND CONCLUSIONS

Our observed differential *HST* counts for ellipticals (E/S0's) and early-type spirals (Sabc's) agree with the simple *no-evolution* model shown here, assuming the LF normalization is correct. Our faintest *HST* counts lie at best marginally above the model predictions. This is consistent with a mildly evolving "giant" galaxy population undergoing a normal rate of star formation (e.g., Bruzual & Charlot 1993). As a caveat to the above, we note that the models described here have been normalized at $b_J = 18.0$ mag. Without this normalization, evolution *is* required in the luminous populations to explain the ~0.3 dex difference between the models and our data. The fact that both populations require the same normalization and that the shape of the observed distribution matches the shape of the models rather well perhaps argues for the case to normalize. *However, until the local predictions of faint galaxy models are reconciled with the local redshift surveys, moderate (local) evolution in the giant galaxy populations cannot be ruled out*. Even so, an agreement within 0.3 dex places the end of the *major* star formation epoch for these types to $z \gtrsim 0.8$, which is consistent with the lack of scale-length evolution observed in *HST* ellipticals out to $z = 0.8$ (Mutz et al. 1994).

The late-type/irregular population shows a considerable discrepancy between the no-evolution predictions and our deep *HST* data. This was also noted by DWG and GL95a down to $I \leq 22.0$ mag, and has now been confirmed down to $m_I \sim 24.25$ mag with a steeply rising—almost Euclidean—slope and *no* indication for a turnover. The *no-evolution* models based on either the LPEM or the MGHC LF fall short of our deep *HST* observations by up to a factor of 10 at the faintest limits. This late-type population is therefore clearly responsible for the "faint blue galaxy excess." Two possible solutions to this discrepancy are (1) strong evolution and/or (2) a serious underestimation of the local space density of dwarf galaxies. The possibility of large-scale nonhomogeneity or a gross error in the cosmological model is ruled out, as the E/S0 and Sabc models fit our *HST* data reasonably well given our basic assumptions. While either of the possibilities considered here can be forced to fit our data, the implications are somewhat unpalatable.[3] If we evolve the widely adopted LPEM LF, then ~2.0 mag of brightening would be required at $z \sim 0.5$ in the *entire* dwarf galaxy population! Alternatively, the additional dwarfs required to explain this population without any evolution result in a significant low-redshift excess in the faint galaxy redshift distributions, which is not observed (GL95a), although the statistics in the redshift surveys are still small and the selection effects formidable. The more recent MGHC LF—based on Zwicky magnitudes—offers a compromise: if the observed steep faint-end LF slope undergoes luminosity evolution, a more reasonable value of ~1.3 mag brightening is implied at $z \sim 0.5$, equivalent to ~2.0 mag in ~20% of the population. The WFPC2 morphological surveys of DWG and GL95a concur that ~40% of the late-type/irregular population shows evidence for recent star formation, while the remaining galaxies appear inert. Together with our deeper *HST* counts, this leads us to conclude that the observed faint blue galaxy excess is caused by a combination of *strong evolution* in a *substantial fraction* of the late-type galaxy population *coupled with* an *underrepresentation* of late-type dwarf galaxies in local surveys (cf. Driver & Phillipps 1995). This "family" of faint galaxy models is explored in detail in Phillipps & Driver (1995).

We thank Doug VanOrsow and Dan Golombek for help in obtaining the data, and Paul Scowen and Barbara Franklin for help in creating the color image. We acknowledge support from *HST* grants GO.5308.01.93A (R. A. W.), .02.93A (W. C. K.), and GO.2684.03.93A (R. A. W.), .01.93A (R. E. G., K. U. R.) and EPSCoR grant EHR-9108761 (W. C. K.).

[3] Note that again *if* normalization of the faint galaxy models at $b_J = 18$ mag is ignored, the problem is amplified by another 0.3 dex.

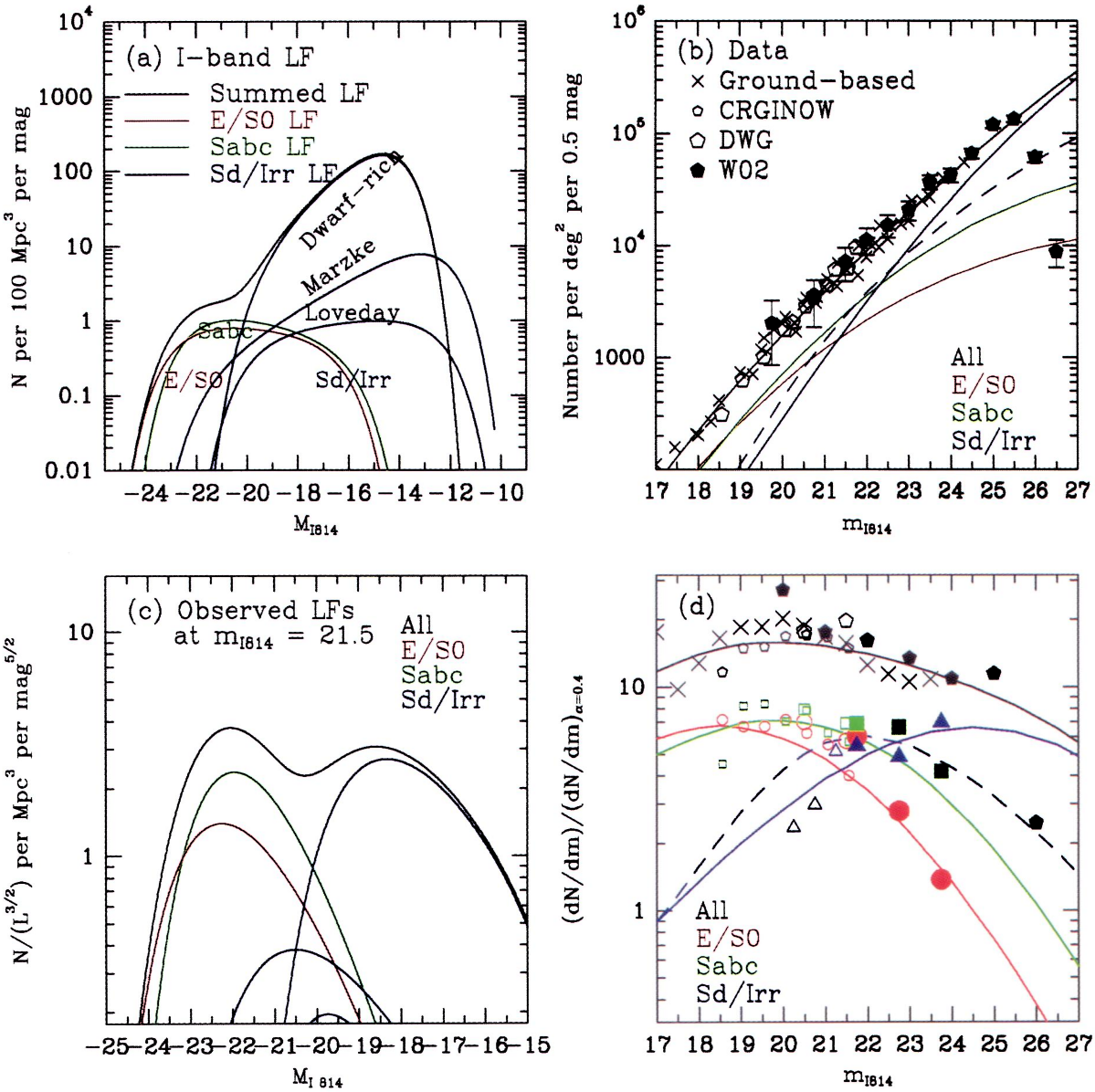

FIG. 3.—(*a*) *I*-band luminosity functions (LFs) used in the morphological modeling. Three variants are shown for the late-type spiral/irregular population: Loveday et al. (1992), Marzke et al. (1994), and Driver et al. (1994). (*b*) Resulting differential *I*-band number counts, along with the best-fit models for each type (*blue solid line*: dwarf-rich case; *blue dashed line*: evolving Marzke LF), as derived from Figs. 2*a*–2*d*. (*c*) As in (*a*), except that the LFs are displayed as they would be observed in a *magnitude-limited* sample. (*d*) Combined *normalized* differential galaxy counts for *all* galaxy types, and for ellipticals and early- and late-type spirals based on our *HST* images. Also shown are the "shallower" data of CRGINOW and DWG, as well as the best-fit models of Figs. 2*a*–2*d*. Note the similarity in shape between the luminosity distributions of the three major galaxy types in (*c*) and their *normalized* differential galaxy counts in (*d*).

REFERENCES

Bahcall, J. N., et al. 1994, ApJ, 435, L51
Broadhurst, T. J., Ellis, & Shanks 1988, MNRAS, 235, 827 (BES)
Bruzual, A. G., & Charlot, S. 1993, ApJ, 405, 538
Casertano, S., Ratnatunga, K. U., Griffiths, R. E., Im, M., Neuschaefer, L. W., Ostrander, E. J., & Windhorst, R. A. 1995, ApJ, in press (CRGINOW)
Driver, S. P. 1994, Ph.D. thesis, Univ. Wales
Driver, S. P., et al. 1994, MNRAS, 266, 155
———. 1995a, in preparation.
Driver, S. P., & Phillipps, S. 1995, ApJ, submitted
Driver, S. P., Windhorst, R. A., & Griffiths, R. E. 1995b, ApJ, in press (DWG)
Glazebrook, K., et al. 1995a, MNRAS, in press (GL95a)
———. 1995b, MNRAS, 273, 157
Griffiths, R. E., et al. 1994, ApJ, 435, L19
Holtzman, J. A., et al. 1995, PASP, 107, 156
Koo, D. C., & Kron, R. G. 1992, ARA&A, 30, 613 (KK92)
Kron, R. G. 1982, Vistas Astron., 26, 37
Lilly, S. J., Cowie, L. L., & Gardner, J. P. 1991, ApJ, 369, 79
Loveday, J., Peterson, B. A., Efstathiou, G., & Maddox, S. J. 1992, ApJ, 390, 338 (LPEM)
Marzke, R. O., Geller, M. J., Huchra, J. P., & Corwin Jr, H. G. 1994, AJ 108, 437 (MGHC)
Mutz, S. B., et al. 1994, ApJ, 434, L55
Neuschaefer, L. W., & Windhorst, R. A. 1995, ApJS, 96, 371
Neuschaefer, L. W., et al. 1995, PASP, in press
Phillipps, S., Davies, J. I., & Disney, M. J. 1990, MNRAS, 242, 235
Phillipps, S., & Driver, S. P. 1995, MNRAS, 274, 832
Ratnatunga, K. U., et al. 1995, in preparation
Schechter, P. 1976, ApJ, 203, 297
Shanks, T., et al. 1984, MNRAS, 206, 767
———. 1989, in The Extragalactic Background Light, ed. S. C. Bowyer & C. Leinert (Dordrecht: Kluwer), 269
Tyson, J. A. 1988, AJ, 96, 1
Windhorst, R. A., et al. 1994a, AJ, 107, 930
———. 1994b, ApJ, 435, 577
Windhorst, R. A., Franklin, B. E., & Neuschaefer, L. W. 1994c, PASP, 106, 798
Windhorst, R. A., & Keel, W. C. 1995, ApJ, submitted (WK)